Lamellar morphologies of melt-crystallized polyethylene, isotactic polypropylene and ethylene–propylene copolymers by the RuO_4 staining technique

Hironari Sano, Takao Usami and Hideaki Nakagawa
Plastics Laboratory, Mitsubishi Petrochemical Co. Ltd, Tohocho-1, Yokkaichi, Mie Prefecture 510, Japan
(Received 8 November 1985; revised 10 December 1985)

The need for staining agents for transmission electron microscope (TEM) studies is widely acknowledged. In this study, lamellar morphologies of melt-crystallized polyethylene (PE), isotactic polypropylene (PP) and ethylene–propylene copolymers have been investigated by extending the technique of ruthenium tetroxide (RuO_4) as a staining agent for the observation of ultra-thin sections using TEM. The excellent image contrast due to Ru made it possible to observe the twisting lamellae of PE and the cross-hatched-type lamellae of PP. The lamellar thicknesses are in good agreement with those derived by the small-angle X-ray scattering method. Some applications of the technique were carried out on the surface structure of injection-moulded PP and the domain structure of ethylene–propylene copolymers.

(Keywords: lamellar morphologies; polyethylene; polypropylene; ethylene–propylene copolymers; transmission electron microscope; RuO_4 staining)

INTRODUCTION

It is well known that many properties of polyethylene (PE) and isotactic polypropylene (PP) depend upon their lamellar morphologies, formed as the result of processing conditions, heat treatment and molecular structure parameters like molecular weight, molecular weight distribution and composition. There exist a variety of lamellar arrangements such as a spherulite, a fibril and a transcrystal. These macrostructure have much influence on toughness, impact strength and fatigue. From these points of view, morphological knowledge of the lamellar structure is indispensable to a fundamental understanding of the properties of PE and PP. However, our morphological knowledge remains far from being sufficiently detailed and, for melt-crystallized PE and PP, still rests largely upon spherulite-scale observation; studies based on lamellar-scale observation are few.

The primary reason for the dearth of lamella-scale observation is that the methods, including the specimen preparation technique, have not been fully developed. There seem to be four methods available so far. First, transmission electron microscopy (TEM) of replicas or scanning electron microscopy (SEM) can be used for the etched sample. Olley *et al.*[1,2], Barnes[3] and Naylar and Phillips[4] applied this method to permanganic acid etched PE and PP. Recently, Norton and Keller[5] observed the cross-hatched lamellae of PP by TEM of replicas for permanganic acid etched samples. Secondly, TEM in defocus image mode[6–8] can be used for unstained ultra-thin sections, but uncontrollable structural changes and damage by radiation can occur and the difficulty of poor image contrast results from the fact that there exist small differences in electron density. Moreover, in preparing ultra-thin sections, the sample must be kept at a very low temperature because the glass transition temperatures (T_g) of PE and PP are about -120°C and -10°C, respectively. Thirdly, high-resolution SEM equipped with the field emission or LaB_6 electron gun made it possible to observe lamellar structures recently[9], but it is generally insufficient to provide necessary information since the observation is limited to the surface and the resolution is unsatisfactorily poor for resolving individual lamellae. Last, TEM for stained ultra-thin sections is considered to be the most appropriate method for the characterization of lamellar structures at a high level of resolution. The Kanig technique[10] using chlorosulphonic acid and uranyl acetate has commonly been used for staining. Grubb and Keller[11] and Strobl *et al.*[12] observed the lamellar structure of PEs by this technique. Recently, Voigt-Martin[13] carried out quantitative evaluation of the distribution of lamella thickness for PEs from TEM results using Kanig's technique. However, it seems to be difficult to apply this technique to PP because degradation of PP proceeds preferentially to staining.

Although osmium tetroxide (OsO_4) is useful for unsaturated polymers[14], a suitable image-contrast-enhancing stain for saturated polymers has been lacking. This situation has been improved somewhat by ruthenium tetroxide (RuO_4) as an effective staining agent for the TEM examination of morphology in both saturated and unsaturated polymeric systems. Trent *et al.*[15] and Montezinos *et al.*[16] recently showed that PE could be stained by RuO_4, but the applicability of RuO_4 as a staining agent for TEM observation of PE and PP is still vague. The purpose of the present study is to

0032-3861/86/091497-08$03.00

investigate the applicability of the technique using TEM for ultra-thin sections stained with RuO_4 to the lamellar morphologies of PE, PP and ethylene–propylene copolymers.

EXPERIMENTAL

Samples

All materials used here are grades of commercial branched low-density polyethylene (BLDPE), linear low-density polyethylene (LLDPE), high-density polyethylenes (HDPEs), isotactic polypropylene (PP) and ethylene–propylene copolymers (co-EPs). The characteristics of these samples are listed in *Table 1*.

Ruthenium tetroxide (RuO_4)

Staining was carried out in the vapour phase. The trimmed specimen embedded in epoxy resin was stained by staying with solid RuO_4 for 10 h in a sealed glass tube.

Sectioning

The amorphous region of the specimen became hard by staining and it was easily sectioned at room temperature. A DuPont Sorvall MT2B type ultramicrotome and a DuPont diamond knife (45°) were used.

Observation of morphologies and characterization of polymers

TEM observation was carried out using a JEOL JEM 100CX instrument. Thermal analysis data were obtained with a Perkin–Elmer DSC-II. Small-angle X-ray scattering (SAXS) and wide-angle X-ray diffraction (WAXD) were measured using a Rigaku RU-200. Infrared (i.r.) spectra were recorded on a Digilab FTS-15C *FT*i.r. system equipped with a mercury–cadmium telluride detector. ^{13}C n.m.r. spectra were obtained at 120°C by a JEOL-FX200 spectrometer equipped with a JEC-980B minicomputer operating in the quadrature detection mode at 50.10 MHz. The pulse width was 45° (9 μs) and the pulse delay was 2 s.

RESULTS AND DISCUSSION

Lamellar morphologies

Figure 1 shows the lamellar morphologies of HDPEs which have different molecular weights. Since the staining medium (RuO_4) penetrates only into the amorphous

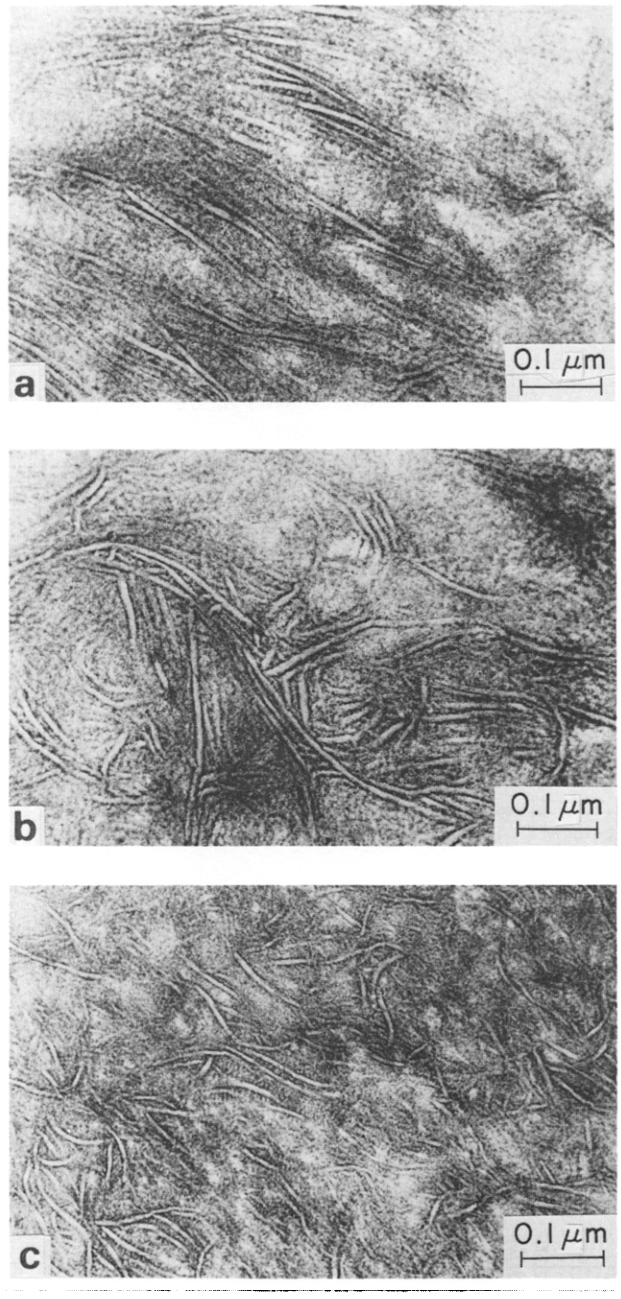

Figure 1 Lamellar morphologies of the different molecular weight HDPEs: (a) outer area of a spherulite of HD-1; (b) central area of a spherulite of HD-1; (c) whole area of a spherulite of HD-3

Table 1 Characteristics of the samples investigated in this work

Sample	$\bar{M}_w$	ρ (g cm^{-3})	[PEP]/total[E] (%)[a]	Stiffness (kg cm^{-2})	Impact (kg cm^{-2})	Remarks
HD-1	7.5×10^4	0.963				
HD-2	1.1×10^5	0.960				
HD-3	9.5×10^5	0.935				
BLDPE	4.5×10^5	0.918				
LLDPE	1.0×10^5	0.920				butene (5 mol%)
PP	3.5×10^5					
LMW-PP	2.2×10^5					
HMW-PP	4.5×10^5					
PP/HDPE blend						PP/HD-1 (8/2)
co-EP-1			3.1	13 100	3.4	
co-EP-2			7.0	12 000	6.1	
co-EP-3			12.6	11 800	6.9	
co-EP-4			18.2	11 600	5.4	

[a] Determined by ^{13}C n.m.r.

regions, the crystalline lamellae appear as white lines and the line widths correspond to the thickness of lamellae. Strong contrast arises when the molecular chain (*c* axis) is parallel to the thin sections; the lamellae cannot be observed when the *c* axis is perpendicular to the thin sections. *Figure 1a* clearly shows that the lamellae have been visualized periodically because lamellae grow twisting along the *b* axis, which is coincident with the radial direction in a spherulite. On the other hand, there are many untwisted and bent lamellae around the centre of a spherulite as observed in *Figure 1b*. They are shorter and thicker than those in the outer area of a spherulite and do not seem to have a fixed growth direction. These bent lamellae have also been observed all over the spherulite of the very high molecular weight PE (HD-3) in *Figure 1c*. For the high molecular weight components, the restriction on the chain diffusion by entanglement impedes the twisting growth of lamellae and, as a result, bent lamellae can be generated.

Figures 2a and *2b* show the lamellar morphologies of BLDPE and LLDPE crystallized at 50°C by cooling at a speed of 1°C min^{-1} from 160°C in d.s.c., respectively. The lamellae of BLDPE and LLDPE are thinner than those of HDPE, and the distributions of thickness and length of lamellae of LLDPE are characteristically wider than those of HDPE and BLDPE, i.e. thick and long lamellae coexist with thin and short lamellae in LLDPE. D.s.c. results showed that LLDPE had a bimodal melting behaviour corresponding to the two kinds of lamellae

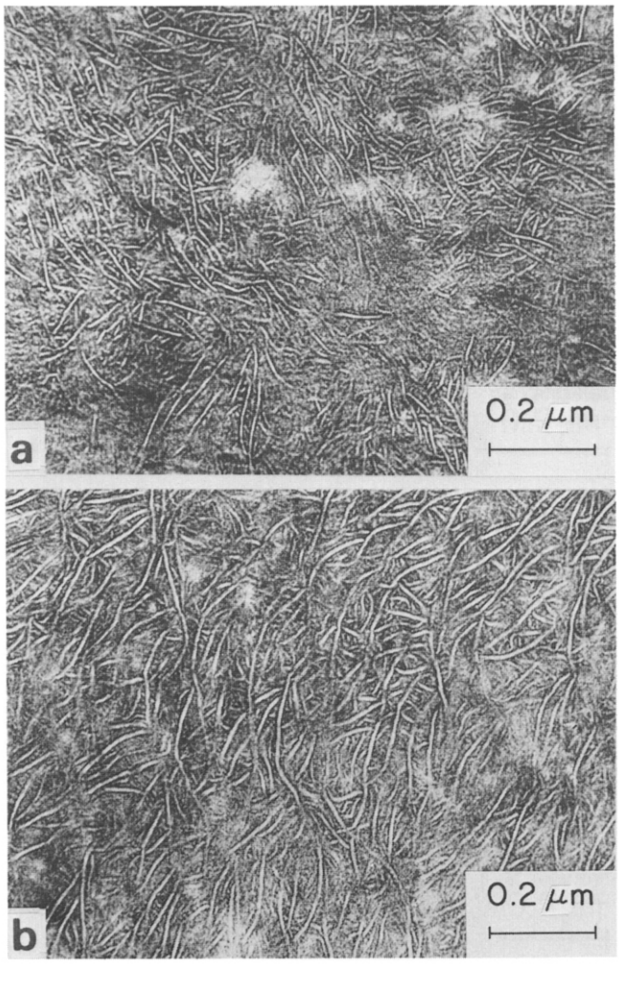

Figure 2 Lamellar morphologies of LDPEs: (a) BLDPE and (b) LLDPE

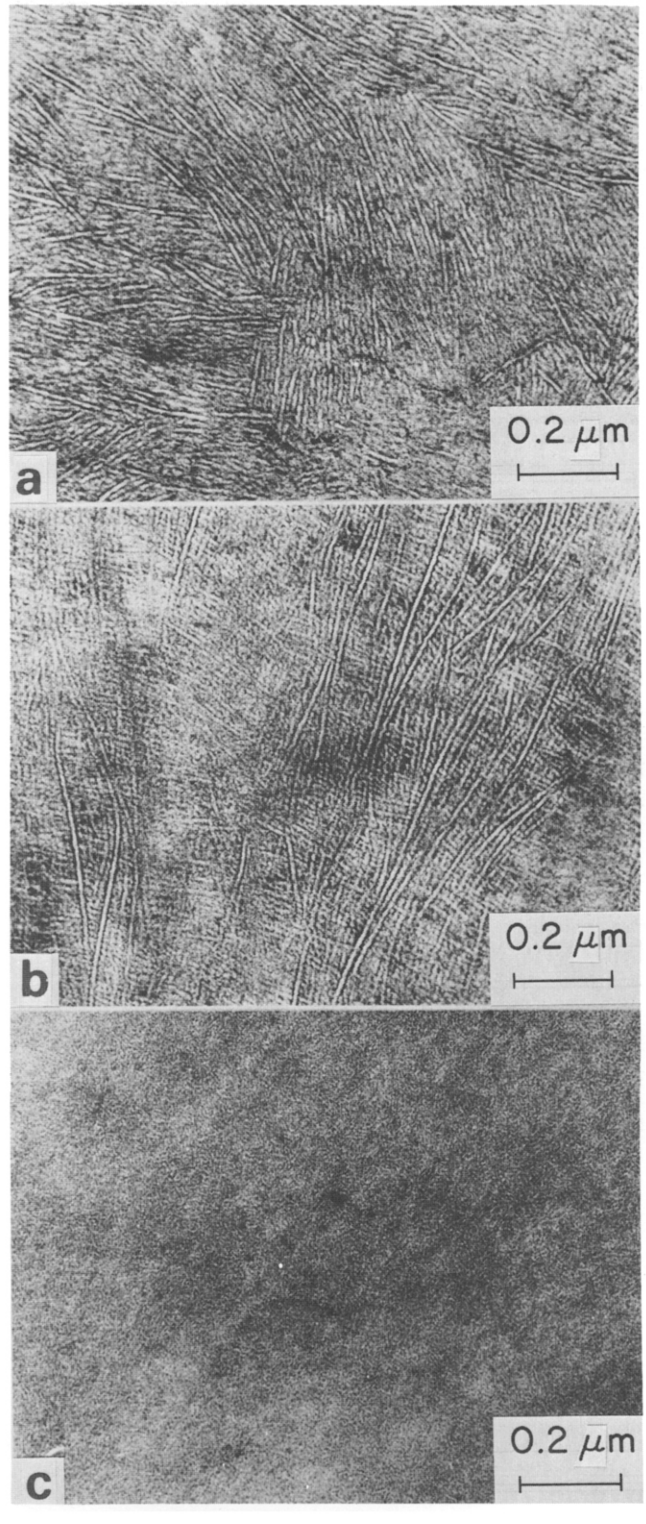

Figure 3 Lamellar morphologies of PP: (a) spherulite of PP; (b) cross-hatched lamellae of PP; (c) nodule-like domain of PP quenched into a dry ice/ethanol bath

mentioned above. This bimodal melting behaviour is considered to be caused by the bimodal distribution of short chain branch contents in LLDPE[17].

The lamellar morphologies of PP crystallized under various conditions are shown in *Figure 3*. *Figure 3a* indicates that the lamellae grow straight along the radial direction in a spherulite without twisting. For PP, lath- and cross-hatched-type lamellar arrangements[18,19] have been reported before and the cross-hatched arrangement is clearly observable in *Figure 3b*. The lamellae of a

PP quenched from the melt into a dry ice/ethanol bath have nodule-like[10,20,21] domain morphology of size ~50 Å as shown in *Figure 3c*, but X-ray diffraction indicated that the nodule-like domain was the result of clustering of microcrystals which could not grow into sheet crystals.

Comparison with other techniques and methods

The morphologies by the RuO_4 staining technique were compared with those by Kanig's technique and the frozen ultra-thin section technique. The thickness of lamellae was also compared with those by d.s.c. and SAXS methods.

Kanig's technique. The morphology of HD-3 by Kanig's technique is shown in *Figure 4a*. The thickness and the arrangement of lamellae are almost the same as those in *Figure 1a*. However, for PP, the specimen was degraded to pieces by the chlorosulphonic acid treatment for 24 h because of molecular chain scission, and the shorter-time treatment could not give a satisfactory stain for TEM observation.

Frozen ultra-thin section technique. Figure 4b shows the lamellar morphology of PP ultra-thin section prepared at −30°C and the morphology is similar to that in *Figure 3a*, although the sharpness and the contrast of the image are different.

D.s.c. The lamellar thickness (l_c) is related to the melting temperature:

$$T_m = T_\infty(1 - 2\sigma_e/l_c\Delta h) \quad (1)$$

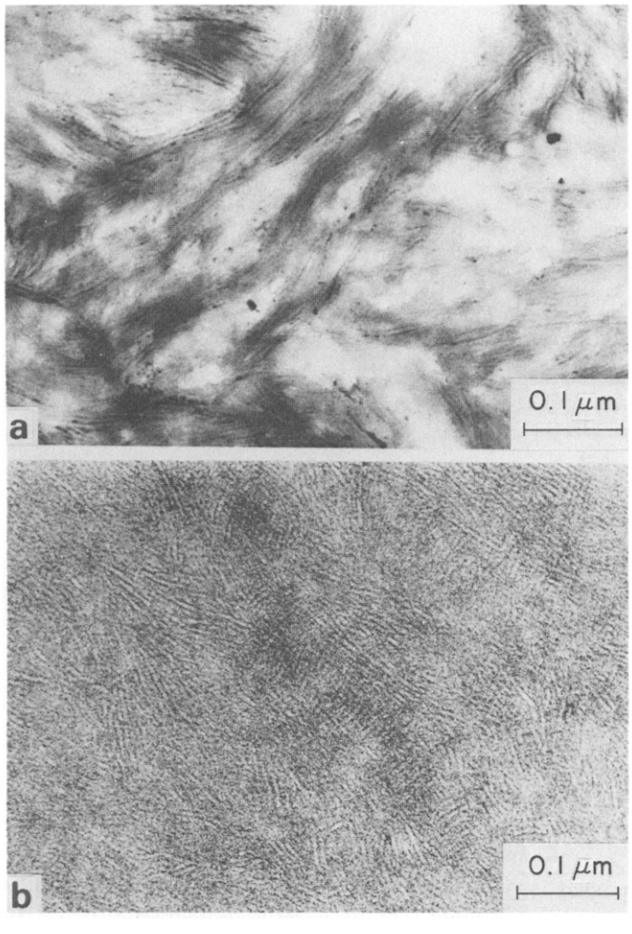

Figure 4 Lamellar morphologies of HD-3 by various techniques: (a) Kanig's technique; (b) frozen ultra-thin section technique

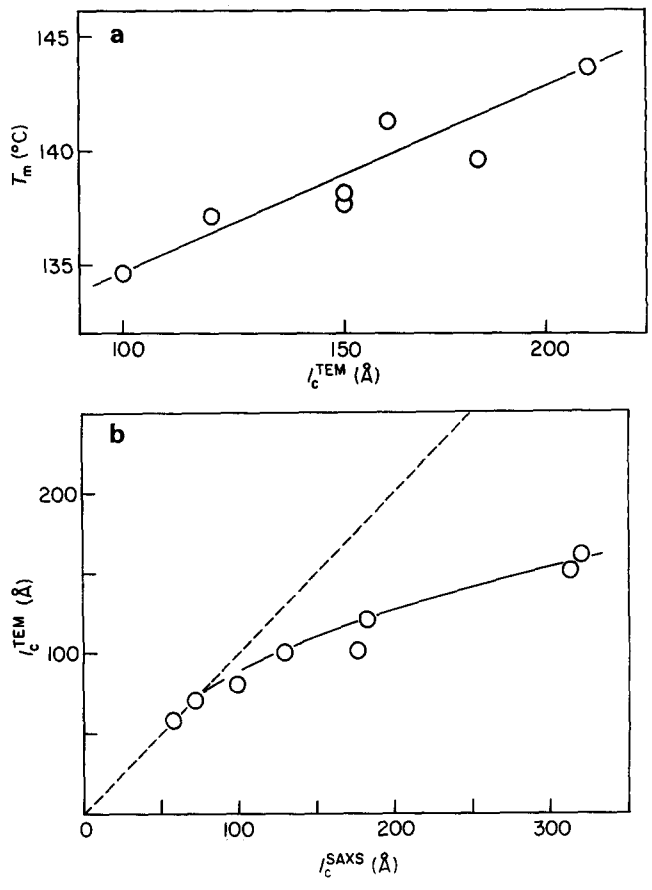

Figure 5 Correlation between the lamellar thickness by the RuO_4 staining technique (l_c^{TEM}) and the results derived by other methods. (a) Correlation between l_c^{TEM} and T_m by d.s.c. for HDPEs. (b) Correlation between l_c^{TEM} and l_c^{SAXS} for all PEs investigated in this work

where T_∞ is the melting temperature of a lamella of infinite thicknes, σ_e is the surface energy of the folded lamella and Δh is heat of fusion. From equation (1), T_m is expected to increase with l_c. Plots of lamellar thickness by the RuO_4 technique (l_c^{TEM}) vs. T_m by d.s.c. for HDPEs gave a satisfactory correlation, as shown in *Figure 5a*.

SAXS. The long spacing (l) can be derived from SAXS measurement using Bragg's equation. The lamellar thickness by SAXS (l_c^{SAXS}) is calculated from the long spacing and the crystallinity (X_c):

$$l_c^{SAXS} = lX_c \quad (2)$$

Plots of l_c^{SAXS} vs. l_c^{TEM} are shown in *Figure 5b* for all PEs investigated in this work. The agreement is quite good in the smaller l_c region, but the l_c^{SAXS} tended to be larger than l_c^{TEM} as l_c increased. The reason is considered to be that the slanting incidence of X-rays to the lamella is expected to given an apparent long spacing longer than the true value for an unoriented sample and the tendency should become more notable in the larger l_c region. Considering this effect, the agreement between l_c^{SAXS} and l_c^{TEM} seems to be good in both small and large l_c regions.

The staining mechanism by RuO_4

RuO_4 staining made sectioning easier and provided strong image contrast for PE and PP. However, the staining mechanism by RuO_4 has not become very clear. From this point of view, the structure changes of PE and PP by RuO_4 staining have been investigated in detail.

Crosslinking. About 50% of the stained PE and PP did not dissolve in *o*-dichlorobenzene at 140°C. The restraint on molecular mobility by crosslinking was so strong that the glass transition temperature (T_g) of ethylene–propylene rubber in its d.s.c. thermogram disappeared after staining. This change of molecular mobility in the amorphous region made PE and PP firmer and easier to section.

I.r. spectra. Structural changes during RuO_4 staining were monitored by i.r. spectra. *Figures 6a* and *6b* show the i.r. spectra of HDPE before and after staining, respectively. The peaks appearing at 1710 cm^{-1}, 1520 cm^{-1} and 580 cm^{-1} can be assigned to carboxylic acid (COOH), carboxylate (COORu) and ruthenium oxide (RuO_x), respectively. Plots of these peak intensities vs. staining time are shown in *Figure 7*. The carboxylic acid appeared earlier than the carboxylate and the total

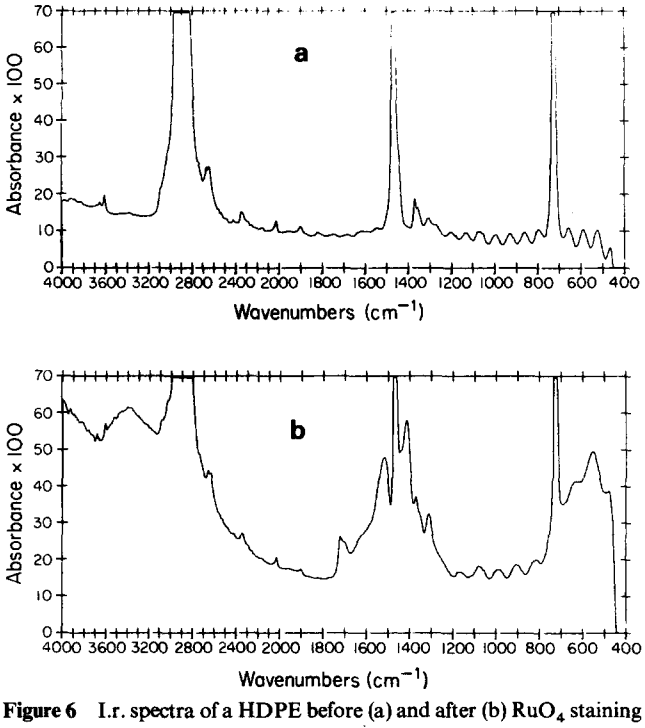

Figure 6 I.r. spectra of a HDPE before (a) and after (b) RuO_4 staining

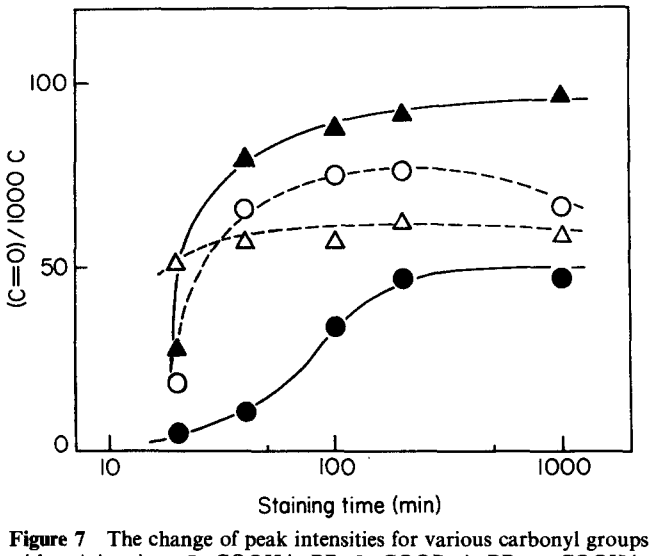

Figure 7 The change of peak intensities for various carbonyl groups with staining time: ○, COOH in PP; ●, COORu in PP; △, COOH in HD-1; ▲, COOR in HD-1

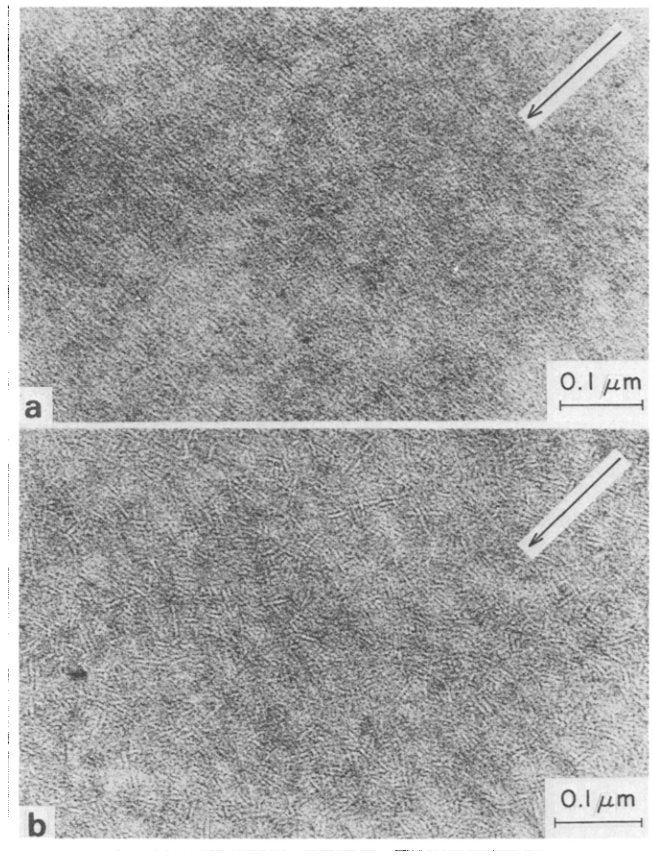

Figure 8 Lamellar morphologies of injection-moulded LMW-PP showing the flow direction (→): (a) skin layer up to 1 μm from the surface; (b) core part

amount of carbonyl groups saturated at 5 h. From these results, oxidation proceeded in PE and carbonyl groups were formed. The appearance of the peaks due to carbonyl groups and the ruthenium oxide indicate that RuO_4 can be converted to RuO_2 by oxidation of the polymer and the RuO_2 can colour the sample and make it harder partly by crosslinking through the carboxylate linkage. For PP, the oxidation behaviour was almost the same as that for PE, but the saturated amount of carbonyl groups was smaller, corresponding to the lower degree of staining. Staining experiments at temperatures above and below T_g (5°C and −25°C) were carried out for PP. The i.r. spectrum showed that oxidation did not proceed below the glass transition temperature. The results indicate that the efficiency of staining depends not on the crystallinity but on molecular mobility in the amorphous region. Therefore, the RuO_4 staining must be carried out above T_g of the polymer.

Crystalline structure. The changes in crystalline structure during staining were monitored by WAXD and SAXS. The crystallinity slightly increased with staining time because of recrystallization at the folded surface, but there was no appreciable effect on l_c by the recrystallization.

Applications

Lamellar morphology in the surface zone of the injection-moulded PP. Injection-moulded PP has the characteristic surface zone called skin. It was found that the surface zone was composed of at least three distinct layers and these layers ranged from a non-spherulitic featureless surface layer to a spherulitic, relatively unstrained central core[22]. However, most studies[22,23] were carried out

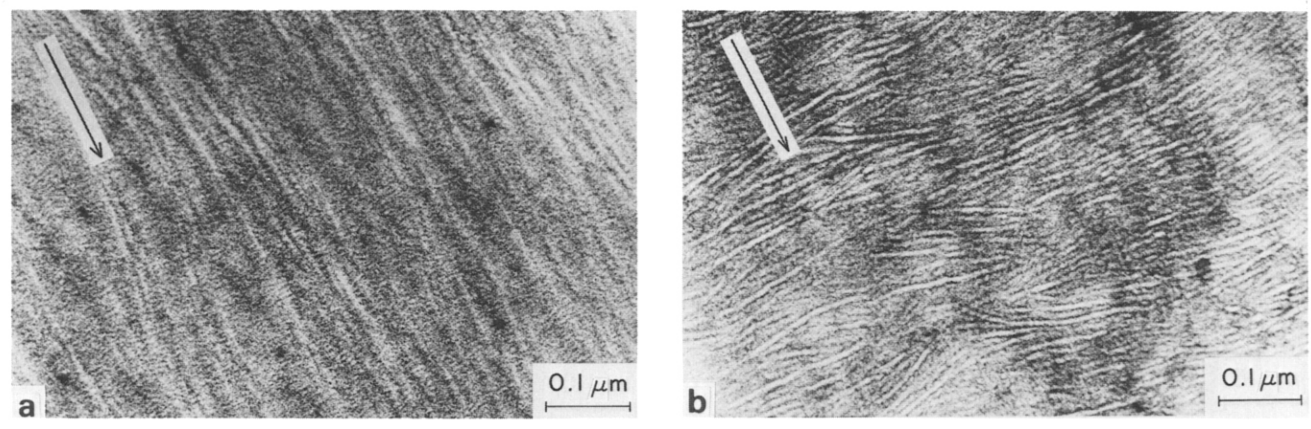

Figure 9 Lamellar morphologies of injection-moulded HMW-PP showing the flow direction (→). (a) skin layer up to 1 μm from the surface; (b) core part

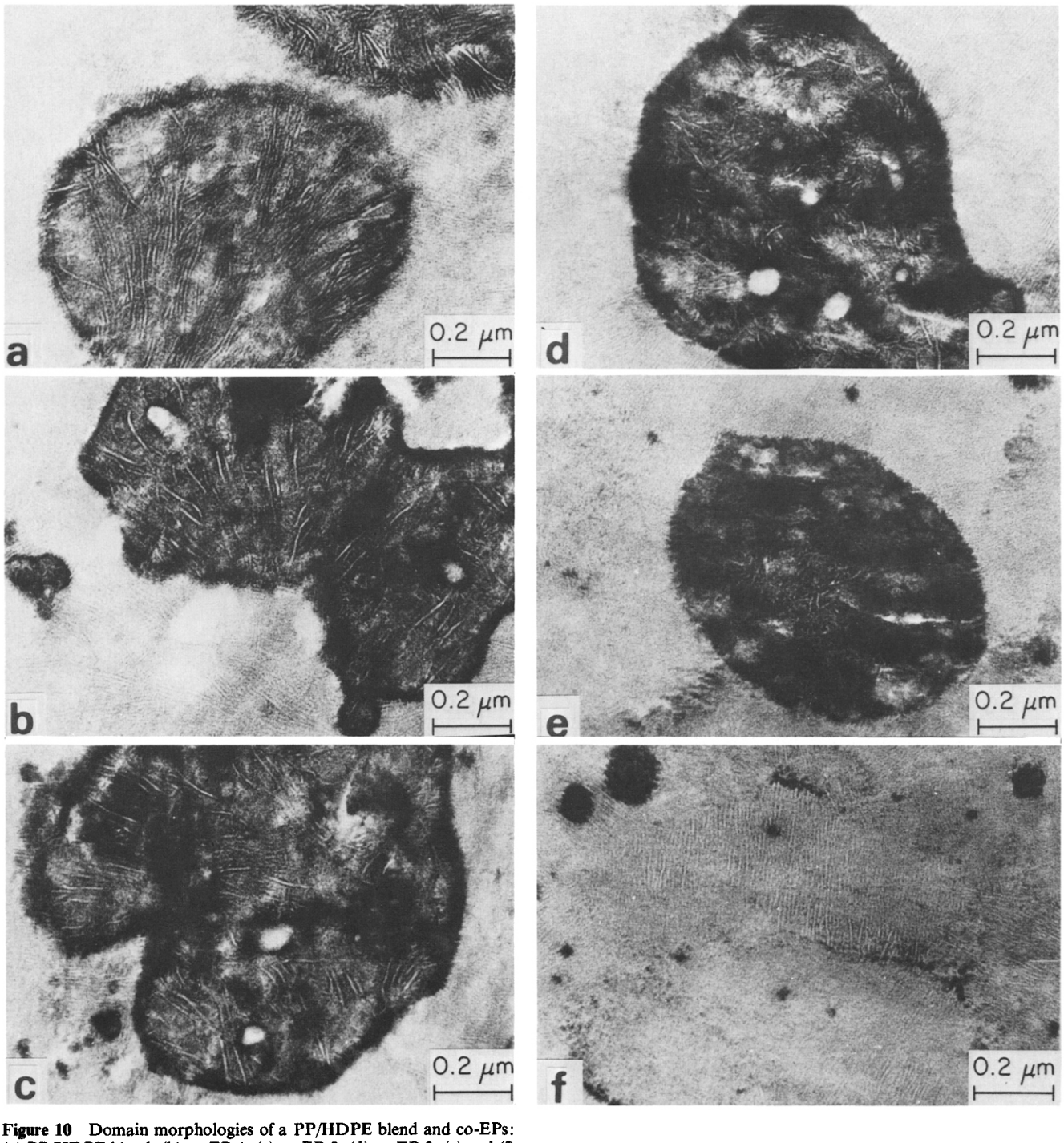

Figure 10 Domain morphologies of a PP/HDPE blend and co-EPs: (a) PP/HDPE blend; (b) co-EP-1; (c) co-EP-2; (d) co-EP-3; (e) and (f) co-EP-4

based on spherulite-scale observation. The RuO_4 staining technique has made it possible to discuss the structure of the surface zone from lamella-scale observation. *Figures 8* and *9* show the depth profiles of the lamellar morphologies for injection-moulded sheets of low molecular weight PP (LMW-PP) and high molecular weight PP (HMW-PP). The skin layer up to 1 μm depth corresponding to the featureless layer by optical microscopy is shown in *Figures 8a* and *9a*. In *Figure 8a*, for LMW-PP, the skin layer is composed of very thin, short lamellae arranged perpendicular to the flow direction, and the thickness and the length are about 50 Å and $\leqslant$ 500 Å, respectively. The core part under the skin is composed of randomly arranged lamellae and the thickness and length increase with depth from the surface, as shown in *Figure 8b*. For HMW-PP, *Figure 9a* shows that long fibrils parallel to the flow direction and lamellae perpendicular to them coexist in the skin. Since these fibrils are hardly stained, it seems that they are composed of highly oriented fibres which have few fold structures. This lamellar arrangement is quite similar to the shish-kebab structure[24-26]. Therefore, it is considered that the very high molecular weight fraction of HMW-PP forms shishes, which act as the nuclei for the following crystallization of lamellae perpendicular to them. The number of shishes decreases remarkably with depth from the surface and there are few shishes at a depth of 50 μm. The lamellae perpendicular to a shish become thicker and longer as the number of shishes decreases, but they are still arranged perpendicular to the flow direction, even at a depth of 50 μm, as shown in *Figure 9b*.

The domain structure of ethylene–propylene copolymers (co-EPs). *Figure 10* shows the domain morphologies of a PP/HDPE blend and four co-EPs. The components of co-EP are PP, PE and ethylene–propylene rubber (EPR)[27]. The four co-EPs are different in their molecular structures depending on the polymerization conditions. The molecular structure characteristics determined by ^{13}C n.m.r. are listed in *Table 1*. *Figure 10a* shows that lamellae of HDPE stay only in the HDPE domain and there is no co-crystallization with PP. For co-EPs, a multilayer domain structure in which PE is surrounded by EPR has been observed as shown in *Figures 10b–f*. As the value of [PEP]/total[E] increases, the domain size becomes smaller and the number of PE lamellae in the domain decreases. Especially for co-EP-4, there are very few lamellae and the dissolution of EPR into PP matrix is visualized as the dark part in the PP matrix. The dissolution of EPR was also confirmed from the shift of the peak temperature and the increase of area in the imaginary component of the complex shear modulus (G'') as shown in *Figure 11*. These morphological differences affect the stiffness and the impact strength of co-EPs as shown in *Table 1*.

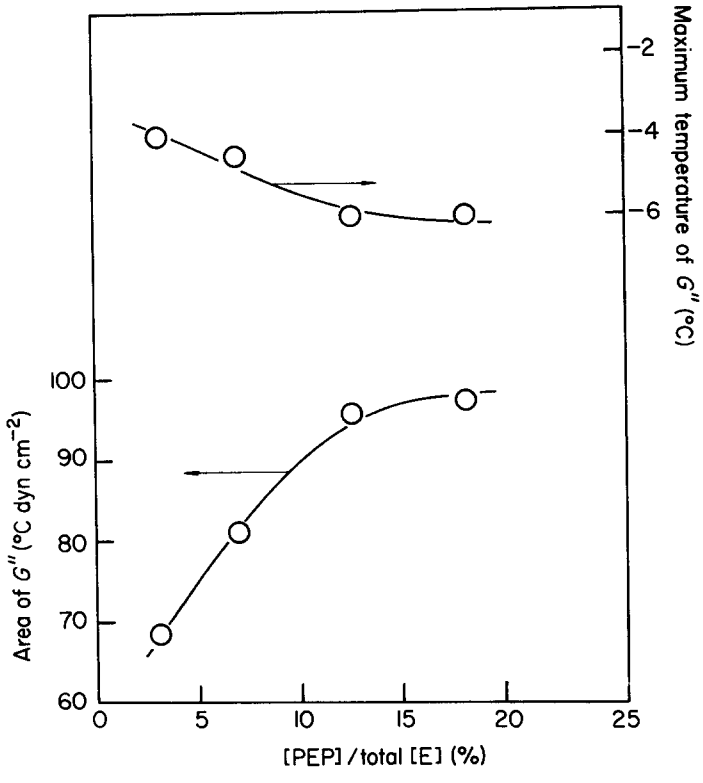

Figure 11 The change of maximum temperature and area of the peak of the imaginary component of the complex shear modulus (G'') with the value of [PEP]/total[E] in co-EPs

CONCLUSIONS

The RuO_4 staining technique was applied to PE and PP in order to observe the lamellar morphologies of ultra-thin section by TEM. The amorphous regions of PE and PP were strongly oxidized and crosslinked to be sectioned easily at room temperature and provide strong image contrast due to the heavy element Ru. Lamellar morphologies such as the twisting lamellae along the radial direction in a spherulite of PE and cross-hatched lamellae of PP are clearly observed. The image has proved to be identical with those observed by other techniques and the lamellar thickness is in good agreement with those determined by d.s.c. and SAXS. The application to injection-moulded PP has shown that there are lamellae even in the skin layer, which appears featureless by optical microscopy, and their structure for HMW-PP is very similar to the shish-kebab structure. For co-EPs, the morphological change depending on their molecular structure difference is clearly visualized and the morphological difference corresponds well to the polymer properties. From these results, it is concluded that the RuO_4 staining technique is very effective and useful for the investigation of lamellar morphologies of PE, PP and their copolymers.

ACKNOWLEDGEMENT

The authors wish to thank Mr John Summers for his assistance in preparing the manuscript.

REFERENCES

1 Olley, R. H., Hodge, A. M. and Bassett, D. C. *J. Polym. Sci., Polym. Phys. Edn.* 1979, **17**, 627
2 Olley, R. H. and Bassett, D. C. *Polymer* 1982, **23**, 1707
3 Barnes, S. R. *Polymer* 1980, **21**, 723
4 Naylar, K. L. and Phillips, P. J. *J. Polym. Sci., Polym. Phys. Edn.* 1983, **21**, 2011
5 Norton, D. R. and Keller, A. *Polymer* 1985, **26**, 704
6 Petermann, J. and Gleiter, H. *J. Polym. Sci., Polym. Phys. Edn.* 1976, **14**, 555
7 Miles, M. J. and Petermann, J. *J. Macromol. Sci.–Phys.* 1979, **B16** (2), 243
8 Roche, E. J. and Thomas, E. L. *Polymer* 1981, **22**, 333
9 Tagawa, T. *J. Polym. Sci., Polym. Phys. Edn.* 1980, **18**, 971
10 Kanig, G. *Colloid Polym. Sci.* 1983, **261**, 373

11 Grubb, D. T. and Keller, A. *J. Polym. Sci., Polym. Phys. Edn.* 1980, **18**, 207
12 Strobl, G. R., Schneider, M. J. and Voigt-Martin, I. G. *J. Polym. Sci., Polym. Phys. Edn.* 1980, **18**, 1361
13 Voigt-Martin, I. G. *J. Polym. Sci., Polym. Phys. Edn.* 1980, **18**, 1513
14 Kato, K. *Polym. Eng. Sci.* 1967, **7**, 38
15 Trent, J. S., Scheinbeim, J. I. and Couchman, P. R. *Macromolecules* 1983, **16**, 589
16 Montezinos, D., Wells, B. G. and Burns, J. L. *J. Polym. Sci., Polym. Lett. Edn.* 1985, **23**, 421
17 Usami, T., Gotoh, Y. and Takayama, S. *Polym. Prepr. Jpn.* 1984, **33**, 2235
18 Bassett, D. C. and Olley, R. H. *Polymer* 1984, **25**, 935
19 Padden, Jr, F. J. and Keith, H. D. *J. Appl. Phys.* 1966, **37**, 4013
20 Lee, S., Miyaji, H. and Geil, P. H. *J. Macromol. Sci.–Phys.* 1983, **B22** (3), 489
21 Reimschuessel, A. C. and Prevorsek, D. C. *J. Polym. Sci., Polym. Phys. Edn.* 1976, **14**, 485
22 Fitchmun, D. R. and Mencik, Z. *J. Polym. Sci., Polym. Phys. Edn.* 1973, **11**, 951
23 Tan, V. and Kamal, M. R. *J. Appl. Polym. Sci.* 1978, **22**, 2341
24 Peterlin, A. *Polym. Eng. Sci.* 1976, **16**, 126
25 Van Hutten, P. F., Koning, C. E., Smook, J. and Pennings, A. J. *Polym. Commun.* 1983, **24**, 237
26 Pennings, A. J., van der Mark, J. M. A. A. and Keil, A. M. *Kolloid Z. Z. Polym.* 1970, **237**, 336
27 Kuroda, T., Fukui, S., Nakagawa, H. and Sano, H. *Polym. Prepr. Jpn.* 1976, **25**, 893